J. Membrane Biol. 162, 139–145 (1998)

The Journal of
Membrane
Biology

Characteristics of a Low Affinity Passive Ca^{2+} Influx Component in Rat Parotid Gland Basolateral Plasma Membrane Vesicles

J.V. Chauthaiwale, T.P. Lockwich, I.S. Ambudkar
Secretory Physiology Section, Gene Therapy and Therapeutics Branch, National Institute of Dental Research, National Institutes of Health, Bethesda, Maryland 20892, USA

Received: 19 March 1997/Revised: 25 November 1997

Abstract. We have previously reported the presence of two Ca^{2+} influx components with relatively high (K_{Ca} = 152 ± 79 μM) and low (K_{Ca} = 2.4 ± 0.9 mM) affinities for Ca^{2+} in internal Ca^{2+} pool-depleted rat parotid acinar cells [Chauthaiwale et al. (1996) Pfluegers Arch. 432: 105–111]. We have also reported the presence of a high affinity Ca^{2+} influx component with K_{Ca} = 279 ± 43 μM in rat parotid gland basolateral plasma membrane vesicles (BLMV). [Lockwich, Kim & Ambudkar (1994) *J. Membrane Biol.* 141:289–296]. The present studies show that a low affinity Ca^{2+} influx component is also present in BLMV with K_{Ca} = 2.3 ± 0.41 mM (V_{max} = 16.36 ± 4.11 nmoles of Ca^{2+}/mg protein/min). Our data demonstrate that this low affinity component is similar to the low affinity Ca^{2+} influx component that is activated by internal Ca^{2+} store depletion in dispersed parotid gland acini by the following criteria: (i) similar K_{Ca} for calcium flux, (ii) similar IC_{50} for inhibition by Ni^{2+} and Zn^{2+}; (iii) increase in K_{Ca} at high external K^+, (iv) similar effects of external pH. The high affinity Ca^{2+} influx in cells is different from the low affinity Ca^{2+} influx component cells in its sensitivity to pH, KCl, Zn^{2+} and Ni^{2+}. The low and high affinity Ca^{2+} influx components in BLMV can also be distinguished from each other based on the effects of Zn^{2+}, Ni^{2+}, KCl, and dicyclohexylcarbodiimide. In aggregate, these data demonstrate the presence of a low affinity passive Ca^{2+} influx pathway in BLMV which displays characteristics similar to the low affinity Ca^{2+} influx component detected in parotid acinar cells following internal Ca^{2+} store depletion.

Key words: Ca^{2+} influx — Parotid gland — BLMV — Kinetics — Divalent cations

Correspondence to: I.S. Ambudkar

Introduction

Stimulation of salivary gland and other nonexcitable cells evokes mobilization of intracellular Ca^{2+}. There is an initial rapid increase in cytoplasmic [Ca^{2+}] ([Ca^{2+}]$_i$), that is due to release of Ca^{2+} from intracellular stores. This is followed by a lower, sustained elevation of Ca^{2+} that is entirely dependent on Ca^{2+} influx across the plasma membrane [1, 3, 16, 19, 21–23]. There are considerable data to support the hypothesis, that the depletion of internal Ca^{2+} stores is the signal that results in the activation of Ca^{2+} influx. Studies with salivary gland and a number of other nonexcitable cells have demonstrated the activation of Ca^{2+} influx upon internal Ca^{2+} store depletion and its inactivation upon internal Ca^{2+} store refill [3, 7, 8, 10, 16, 23]. However, the mechanism(s) by which internal Ca^{2+} store depletion activates the Ca^{2+} entry process in parotid gland and other nonexcitable cells is not yet known. We have recently demonstrated the presence of two Ca^{2+} influx components in internal Ca^{2+} store-depleted parotid acinar cells with distinct affinities for Ca^{2+} (K_{Ca} 152 ± 79 μM and 2.4 ± 0.9 mM, respectively) [2, *also see* Table 1]. While the high affinity component we have reported has not been previously described in any other cell type, a Ca^{2+} influx component with similar K_{Ca} as the low affinity component in parotid acini, has been reported following internal Ca^{2+} store depletion in T lymphocytes [4]. A similar K_{Ca} has also been reported for I_{CRAC}, a Ca^{2+} current activated in response to internal Ca^{2+} store depletion in rat mast cells [9]. In addition, several distinct divalent cation entry channels are also activated in the mast cells under these conditions [5, 6]. However the molecular nature of the components in the plasma membrane that mediate Ca^{2+} influx, activated via internal Ca^{2+} store depletion or any other mechanisms, has not yet been described in any nonexcitable cell tupe.

Unlike voltage-gated Ca^{2+} channels that have been well characterized based on their reactivity towards specific drugs, toxins, and divalent cations [3], the Ca^{2+} influx pathways in nonexcitable cells have not been reported to be modified by any specific pharmacological compound. This lack of a specific ligand has hindered progress in the identification and purification of the protein(s) that mediate Ca^{2+} influx in these cell types. In an efffort to determine the biochemical and molecular characteristics of the Ca^{2+} entry pathways in rat parotid cells, we have studied the passive Ca^{2+} permeability of isolated basolateral plasma membrane vesicles (BLMV). Our previous studies demonstrate that $^{45}Ca^{2+}$ influx in BLMV has characteristics similar to those of divalent cation entry in dispersed rat parotid acinar cells [12–14]. Divalent cation entry in both cases is affected by factors such as the Ca^{2+} gradient across the plasma membrane, membrane potential, dicyclohexylcarbodiimide (DCCD), pH, [Ca^{2+}] on cytoplasmic side of membrane, and is inhibited by Ni^{2+} and Zn^{2+}. Further, we have described the presence of a relatively high affinity, trypsin-sensitive, passive Ca^{2+} influx component in BLMV with characteristics, such as K_{Ca} and inhibition by low temperature and DCCD, which are similar to those of the high affinity Ca^{2+} influx component detected in internal Ca^{2+} pool-depleted rat parotid acinar cells [12].

As discussed above, Ca^{2+} influx activated in response to internal Ca^{2+} store depletion, has been suggested to be mediated via a relatively low affinity component in T-lymphocytes and mast cells. We have recently reported the presence of a similar, low affinity Ca^{2+} influx component in internal Ca^{2+} store-depleted rat parotid gland parotid acinar cells [2]. In the present study we have demonstrated for the first time the presence of a saturable low affinity, passive Ca^{2+} influx component in BLMV, with K_{Ca}, and other characteristics, similar to that of the low affinity Ca^{2+} influx component in internal Ca^{2+} store-depleted parotid acinar cells.

Materials and Methods

The animals used in these studies were male Wistar rats that were obtained from Harlan Sprague-Dawley. Hank's Balanced Salt Solution was purchased from Gibco BRL and fura-2/AM, thapsigargin, mannitol and dithiothreitol (DTT) from Calbiochem. CLPSA collagenase was obtained from Worthington and lima bean trypsin inhibitor, hyaluronidase, bovine serum albumin, N,N′-dicyclohexylcarbodiimide (DCCD) and phenylmethylsulfonyl fluoride (PMSF) were obtained from Sigma Chemicals. $^{45}CaCl_2$ (2 mCi/ml) was obtained from Amersham. Percoll was purchased from Pharmacia. Protein concentration was determined by using the Bio-Rad protein assay kit (Bio-Rad Laboratories) with bovine serum albumin as standard.

Cell Preparation and Fura-2 Loading

Dispersed parotid acinar cells were prepared by collagenase and hyaluronidase digestion as described previously [2, 16]. Briefly, cleaned and minced rat parotid glands were incubated in Hank's Balanced Salt Solution containing HEPES buffer (HBSS medium) for 80 min at 37°C with CLPSA collagenase (300–400 U/ml) with gassing (95% O_2 + 5% CO_2) every 20 min. After this incubation, the suspension was thoroughly washed with HBSS and incubated with fura-2/AM (2 μM) and lima bean trypsin inhibitor (1 mg/10 ml) at 30°C for 45 min. The cells were then washed three times with HBSS and resuspended in HBSS with lima bean trypsin inhibitor and maintained at 30°C till use. Depletion of internal Ca^{2+} stores was achieved by treating the cells with thapsigargin (2 μM) at 30°C for 20 min in HBSS containing 1.28 mM Ca^{2+}.

Fluorescence Measurements

Fura-2 fluorescence was measured using a SLM 8000-DMX1000 spectrofluorimeter as previously described [2]. Before each assay cells were gently pelleted at 400 × *g*, washed two times with nominally Ca^{2+}-free HBSS medium, resuspended in the same medium and kept gently stirred in a cuvette maintained at 37°C. The excitation and emission wavelengths were 340 nm, 380 nm and 510 nm, respectively. Cytoplasmic [Ca^{2+}] ([Ca^{2+}]$_i$) was calculated as described previously [2]. Required amount of $CaCl_2$ was added to thapsigargin-treated cells to initiate Ca^{2+} influx; 250 μM for the high affinity component and 5.0 mM for the low affinity component. After addition of $CaCl_2$, the changes in [Ca^{2+}]$_i$ during the first 5 min were monitored (data collected every 0.3 sec). The initial rate of increase in [Ca^{2+}]$_i$ after addition of Ca^{2+} to the extracellular medium was calculated by nonlinear regression analyses of the [Ca^{2+}]$_i$ values obtained within the first 100 sec for lower [Ca^{2+}] and between 5–20 sec for higher [Ca^{2+}]. Similar values were obtained from a polynomial or double rectangular hyperbola fit of the data. The initial rate of change of [Ca^{2+}]$_i$ under these conditions can be used as a measure of the rate of Ca^{2+} influx [2, 4].

Preparation of BLMV

BLMV were prepared as previously described [11, 12]. Briefly, parotid glands from 10–12 male Wistar rats (Sprague-Dawley, 150–200 grams) were excised, cleaned, and homogenized in a medium containing 250 mM sucrose, 10 mM Tris-HCl (pH 7.5), 1 mM DTT, and 0.1 mM phenylmethylsulfonyl fluoride. The homogenate was centrifuged at 3,000 × *g* for 15 min to remove cell debris. The resulting supernatant was centrifuged at 23,500 × *g*. The pellet was resuspended in the homogenization medium, mixed with Percoll (12% v/v) and centrifuged at 49,000 × *g* for 30 min. The BLMV fraction was collected and washed three times with (in mM): 100 mannitol, 1 DTT, 0.1 PMSF, and 10 Tris-HCl, pH 7.5. The final pellet was suspended in 300 mannitol, 1 DTT, and 10 Tris-HEPES (pH 7.4) at a concentration of 1–3 mg protein/ml, aliquoted, and frozen in liquid N_2, and stored at −70°C until use (maximum two weeks). Before use, aliquots of BLMV were thawed on ice; all preparations were subjected to only one freeze-thaw cycle.

DCCD-Treatment of BLMV

100 μg/ml of BLMV were pretreated for 20 min with 2 mM DCCD in 10 mM Tris-Hepes (pH 7.4) and 1 mM $MgCl_2$ at 37°C. The reaction was stopped after 20 min by putting the tube on ice. The DCCD-treated BLMV were then separated from the reaction media by centrifugation (106,000 × *g*, 20 minutes, 4°C). The resultant pellet was rehomogenized in 10 mM Tris-Hepes (pH 7.4), 1 mM $MgCl_2$ and used for ^{45}Ca flux measurements described below. Control BLMV, treated with the vehicle (DMSO) only, were prepared at the same time.

^{45}Ca FLUX INTO BLMV

$^{45}Ca^{2+}$ influx into BLMV was measured as described earlier [12–14]. Uptake was initiated by addition of $^{45}Ca^{2+}$ to 10 μg of BLMV in 100 μl of assay medium containing 10 mM Tris-Hepes (pH 7.4), 2 mM $MgCl_2$. Under these conditions, there is no ATP-dependent Ca^{2+} transport, or Na^+/Ca^{2+} exchange, activity in BLMV. Ca^{2+} influx through high and low affinity components was studied by using Ca^{2+} at 50 μM and 7.5 mM, respectively. After incubation for 5 sec at 30°C, ice-cold stop buffer containing 10 mM Tris-HEPES (pH 7.4), 2.5 mM $MgCl_2$ and 0.35 mM $LaCl_3$ was added. The mixture was filtered through Millipore filters (0.45μ, type HA) using a Millipore filtration system and washed three times (3 ml each) with ice-cold stop. The filters were then dried, dissolved in Aquasol (DuPont) and the radioactivity determined using a scintillation counter (Hewlett-Packard, Tricarb). To determine background $^{45}Ca^{2+}$ uptake, i.e., at 0 sec, stop buffer was added to BLMV prior to addition of $^{45}Ca^{2+}$. Kinetics of Ca^{2+} entry in depolarized BLMV was studied by adding 50 mM KCl to 10 μg BLMV in 100 μl just before addition of $^{45}Ca^{2+}$ (0.5–10 mM). Initial rates of Ca^{2+} uptake (nmoles Ca^{2+}/mg protein/minute) at various [Ca^{2+}] were calculated from the uptake in the first 5 sec. The data in the manuscript have been presented as mean ± SEM for the number of experiments indicated in the figure legends. Where indicated, the Student's T-Test was used to statistically evaluate the data.

ABBREVIATIONS

BLMV, basolateral membrane vesicles; DCCD, N,N′-Dicyclohexylcarbodiimide; HEPES, 4-(2-hydroxyethyl)-1-piperizineethanesulfonic acid; DMSO, dimethylsulfoxide; DTT, dithiothreitol; PMSF, phenylmethylsulfonic acid.

Results and Discussion

KINETICS OF Ca^{2+} ENTRY INTO BLMV AT 30°C

Figure 1*A* shows the rate of Ca^{2+} entry into BLMV at 30°C as a function of the [Ca^{2+}] in the assay. Initial rates of Ca^{2+} influx into BLMV were calculated by measuring $^{45}Ca^{2+}$ uptake as described in Materials and Methods. The rate of Ca^{2+} influx increases with increasing extravesicular [Ca^{2+}] and saturates as [Ca^{2+}] approaches 10 mM. Nonlinear regression analysis of these data shows the presence of two saturable Ca^{2+} influx components with distinct low and high affinities for Ca^{2+}, K_{Ca} = 2.3 ± 0.41 mM and 283 ± 93 μM, respectively (V_{max} = 16.36 ± 4.11 nmoles Ca^{2+}/mg protein/min and 3.22 ± 0.75 nmoles Ca^{2+}/mg protein/min, respectively). An Eadie Hofstee plot of these data is shown in Fig. 1*B*. The nonlinear pattern of this plot, and the kinetic parameters calculated for the two components from this plot, are consistent with the values obtained by nonlinear regression of the data. Similar values were obtained with BLMV isolated from a dispersed cell preparation of rat parotid glands (*data not shown*). Results presented in the following sections were obtained with BLMV isolated from homogenized glands. In this case the yield of BLMV was higher than when prepared from an enzymatically dispersed cell preparation.

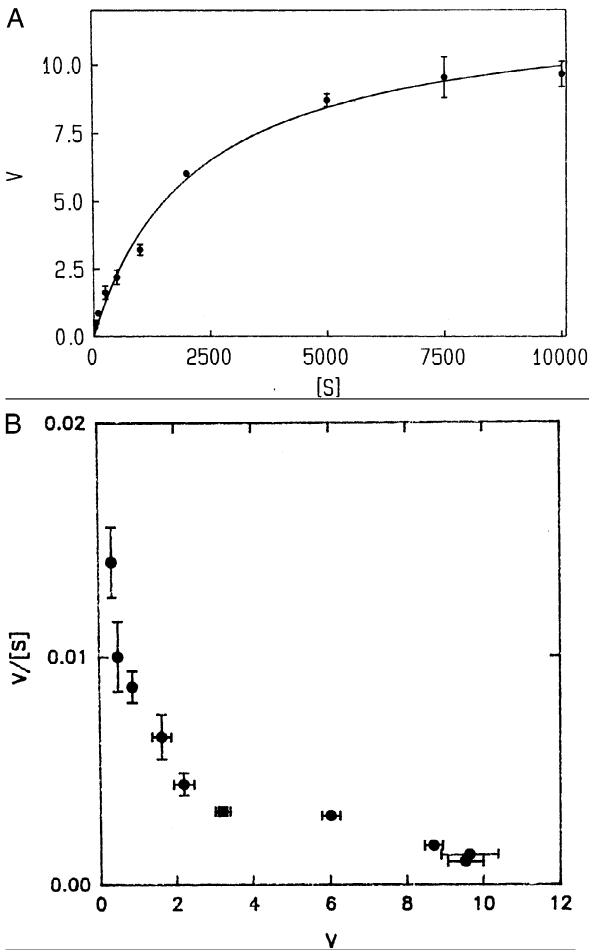

Fig. 1. Kinetics of Ca^{2+} entry in BLMV. Initial rates of $^{45}Ca^{2+}$ influx into BLMV at various [Ca^{2+}] were measured using the Millipore filtration method as described in Materials and Methods. Rate of Ca^{2+} entry (velocity *V*, nmoles Ca^{2+}/mg protein/minute) as a function of extravesicular [Ca^{2+}] ([S], in μM) is shown in Fig. 1*A*. Data are shown as mean ± SEM from 3–4 experiments with different BLMV preparations. Kinetic parameters were determined by nonlinear regression analysis of the data and are given in Table 1. Fig. 1*B* shows the Eadie-Hoffstee plot of the data.

The values for the high affinity Ca^{2+} influx component obtained here are similar to that reported by us earlier [12, 14, *also see* Table 1]. It is likely that in our earlier studies the low affinity site was not detected since; (i) a relatively high capacity nonsaturable (leak) pathway for Ca^{2+} masked the saturable low affinity component, and (ii) higher (i.e., >1.0 mM) concentrations of Ca^{2+}, which are required to detect the low affinity component, likely induced fusion of BLMV (detected as increase in steady-state levels of Ca^{2+} uptake). In the present studies, Ca^{2+} influx assays were performed at relatively low temperature 30°C instead of 37°C to decrease Ca^{2+} flux via the unsaturable Ca^{2+} influx component and

Table 1. K_{Ca} for different Ca^{2+} entry components

Cell type	K_{Ca}		Reference
	High affinity	Low affinity	
	(μM)	(mM)	
Rat parotid acinar cells:			
Unstimulated	ND	3.4 ± 0.7	[2]
Internal Ca^{2+} pool-depeleted	152 ± 79	2.4 ± 0.9	[2]
BLMV	283 ± 93	2.3 ± 0.41	Present studies
Rat mast cells	ND	3.3	[9]
Jurkat T-cell line	ND	3.3	[4]

ND: not detected

minimize the effects of high [Ca^{2+}] on vesicle fusion. Importantly, the present experimental approach has demonstrated the presence of a low affinity Ca^{2+} influx site in BLMV. Studies previously reported by Hoth and Penner [9] and Donnadieu et al. [4] and us [2] have demonstrated that a relatively low affinity Ca^{2+} entry component is present in mast cells, T lymphocytes, and parotid gland cells, respectively, and contributes towards Ca^{2+} influx into these cells following internal Ca^{2+} store depletion (*see* Table 1). To our knowledge, this is the first report showing the presence of a similar low affinity passive Ca^{2+} influx component in isolated plasma membrane vesicles from a nonexcitable tissue. Below we describe the characteristics of this low affinity component in BLMV.

Effect of Divalent Cations Ni^{2+} and Zn^{2+} on Ca^{2+} Influx Via the Low Affinity Component in BLMV and Parotid Acini

To compare the low affinity Ca^{2+} component in BLMV with that in dispersed parotid acini we have examined the inhibitory effects of Ni^{2+} and Zn^{2+} on Ca^{2+} influx via these components. Ni^{2+} is an efficient blocker of Ca^{2+} influx in salivary and other nonexcitable cells, while a low concentration of Zn^{2+} has been shown to inhibit depletion-activated Ca^{2+} influx [3, 8, 15]. The low affinity Ca^{2+} influx components in cells and BLMV, were measured with 5 mM Ca^{2+} in the medium (either extracellular or extravesicular). Figure 2 shows the effects of Ni^{2+} and Zn^{2+} on calcium influx in BLMV (*A*) and on cells (*B*). Ni^{2+} and Zn^{2+} used were in the range of 0.5–5.0 mM in either case. A similar pattern of inhibition of $^{45}Ca^{2+}$ flux in BLMV is obtained with either Ni^{2+} or Zn^{2+}, with a maximum inhibition of 70–80% induced by either cation. Both divalents also inhibit Ca^{2+} influx into intact acini (maximum inhibition is about 80%) although, there is slightly more inhibition by Zn^{2+} than Ni^{2+}. Importantly, the IC_{50} values calculated for each cation, for inhibition of Ca^{2+} entry via the low affinity components in either BLMV or cells are similar (Table 2). In contrast, the high affinity site in cells displays a very high sensitivity to Zn^{2+} (IC_{50} = 5.68 ± 1.19 μM) as compared to Ni^{2+} (IC_{50} = 49.0 ± 5.78 μM) (*data not shown*).

Effect of KCl on the Kinetics of the Low Affinity Ca^{2+} Entry Component in BLMV

Although Ca^{2+} influx into nonexcitable cells is not a voltage-activated process, membrane depolarization has been shown to induce a decrease in the level of Ca^{2+} influx in salivary and other cells [9, 17, 24]. We have recently reported that depolarization of rat parotid acini with KCl (50 mM) induces an increase in the K_{Ca} of the low affinity Ca^{2+} influx component (from 2.4 ± 0.9 mM to 4.9 ± 0.69 mM) without any change in V_{max} [2]. Here we have examined the kinetics of Ca^{2+} influx into BLMV in the presence of 50 mM KCl in the medium and the results are shown in Fig. 3. The rate of Ca^{2+} influx into BLMV at [Ca^{2+}] < 10 mM is lower in the presence of KCl than its absence (*see* Fig. 1). However, as [Ca^{2+}] approaches 10 mM, there is no detectable difference in the rates of Ca^{2+} influx in either condition. Nonlinear regression analysis of the data demonstrate that depolarization induces a significant increase in K_{Ca} of the low affinity Ca^{2+} influx component from 2.3 ± 0.41 mM to 4.28 ± 0.76 mM ($P < 0.05$), without any significant change in V_{max}. These KCl-induced changes in the Ca^{2+} influx components can also be seen in the Eadie Hoffstee plot of the data (*see* inset Fig. 3). These data suggest that KCl exerts an apparent noncompetitive type of inhibitory effect on the low affinity Ca^{2+} influx components in rat parotid gland BLMV and acini.

Effect of pH on Ca^{2+} Influx Via the Low Affinity Ca^{2+} Influx Components in Parotid Acini and BLMV

Ca^{2+} influx in parotid and pancreatic acinar cells has been reported to be modulated by extracellular pH [13,

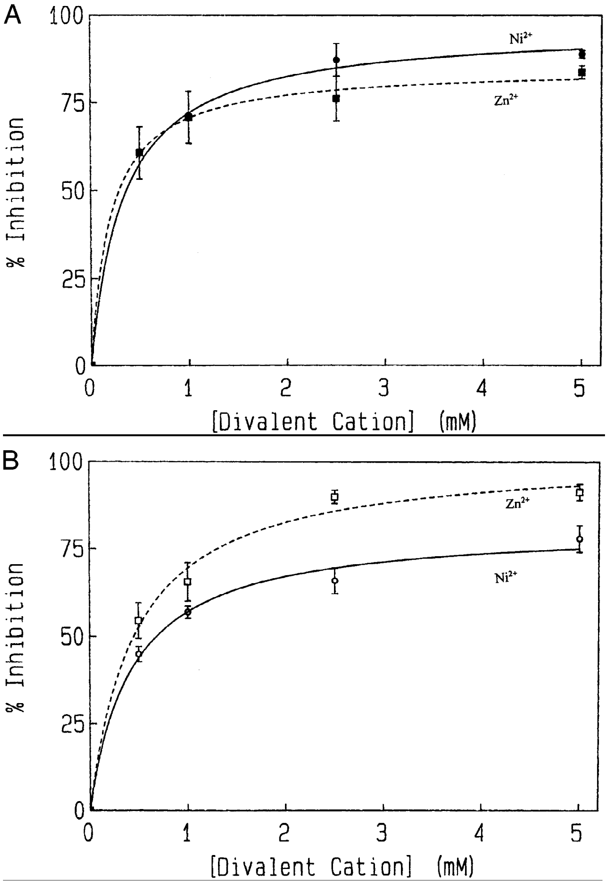

Fig. 2. Effect of Ni^{2+} and Zn^{2+} on the low affinity Ca^{2+} influx components in internal Ca^{2+} pool-depleted cells and BLMV. (*A*) $^{45}Ca^{2+}$ (5 mM) was added to BLMV (10 μg, in assay buffer) in presence of Ni^{2+} (filled circles) or Zn^{2+} (filled squares) (0.5 to 5.0 mM). The rate of Ca^{2+} uptake was calculated as described in Materials and Methods. Inhibition of uptake at various divalent concentrations (expressed as % maximum inhibition) is shown. (*B*) Ni^{2+} (open circle) or Zn^{2+} (open squares) (0.5 to 5.0 mM) was added to internal Ca^{2+} pool-depleted cells, prior to addition of Ca^{2+} (5.0 mM). The changes in $[Ca^{2+}]_i$ during the first 5 min were monitored. Initial rates of calcium entry were calculated by nonlinear regression analyses of values obtained within 20 sec. The extent of inhibition (expressed as % of maximum inhibition) as a function of concentration of divalent cation is shown. The data shown are mean ± SEM of 3–4 experiments.

19]. Figure 4 shows the effect of pH on Ca^{2+} influx via the low affinity Ca^{2+} influx component in parotid acinar cells and BLMV. In both cases, low pH (6.6) induces a similar decrease (aout 50%) in the rate of Ca^{2+} influx while elevated pH (8.2) has no effect. These results further demonstrate the similar characteristics of the low affinity Ca^{2+} influx components in parotid cells and BLMV. In contrast, the high affinity Ca^{2+} influx component in cells is decreased by low pH and increased by elevated pH, consistent with our previous report showing the effects of pH on Mn^{2+} entry into parotid acini [13]. These results suggest that the high and low affinity Ca^{2+}

Table 2. IC_{50} values for divalent cation inhibition of the low affinity Ca^{2+} influx component

	BLMV	Cells
Ni^{2+} (mM)	0.25 ± 0.05	0.25 ± 0.03
Zn^{2+} (mM)	0.32 ± 0.01	0.4 ± 0.08

Inhibition of a low affinity Ca^{2+} entry component ($[Ca^{2+}] = 5.0$ mM) by divalent cations was studied. The concentration range of Ni^{2+} and Zn^{2+} used was 0.5 to 5.0 mM. IC_{50} values were calculated from plots shown in Fig. 2. Student's *t*-Test was used to evaluate the data. The values obtained for Ni^{2+}, and Zn^{2+}, for BLMV and cells, respectively, are not significantly different from each other.

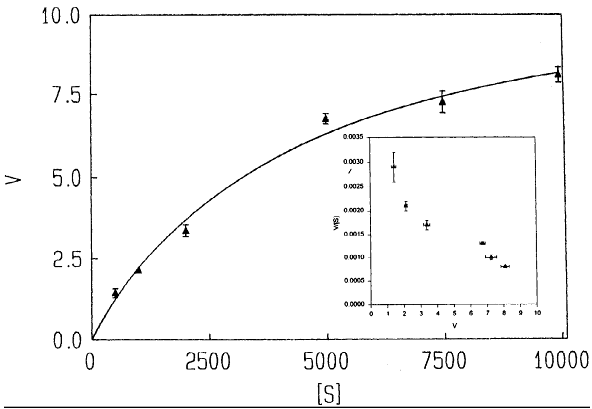

Fig. 3. Kinetic analysis of Ca^{2+} influx (low affinity) in depolarized BLMV. BLMV (10 μg) suspended in assay buffer (*see* Materials and Methods) were incubated with 50 mM KCl 10 sec prior to addition of $^{45}Ca^{2+}$ (0.5 to 5.0 mM). Ca^{2+} uptake was carried out at 30°C for 5 sec. The rate of Ca^{2+} was calculated as described earlier. Rate of Ca^{2+} entry (*V;* nmoles of Ca^{2+}/mg protein/min) is plotted against extravesicular $[Ca^{2+}]$. ([S], in μM). Kinetic parameters were calculated by nonlinear regression analysis of the data. An Eadie Hoffstee plot of the data is shown in the Inset. Data shown are mean ± SEM for 3–4 experiments.

influx components detected in the cells have distinct characteristics. However, unlike in cells, the high affinity Ca^{2+} influx component in BLMV is not increased at pH > 7.4 (*also see* our previous report) [13]. Although we cannot fully explain this difference in the responses of the high affinity Ca^{2+} influx components in cells and BLMV to elevated pH, we have previously reported, that these two Ca^{2+} influx components display several other similar characteristics (12–14).

Distinct Characteristics of the High and Low Affinity Ca^{2+} Influx Components in BLMV

The data presented above indicate that the high and low affinity Ca^{2+} influx components in BLMV have different characteristics. To further examine the two Ca^{2+} influx components we have compared the effects of DCCD and

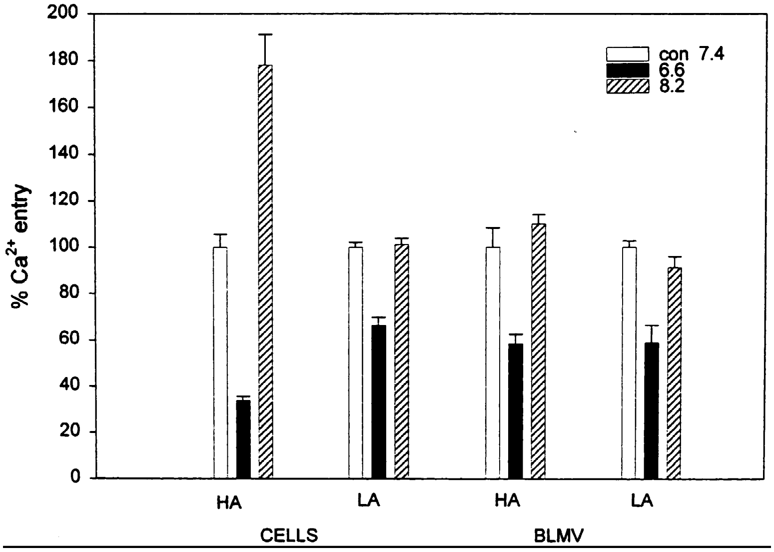

Fig. 4. Effect of pH on Ca^{2+} via the low affinity component in BLMV and parotid acini. BLMV (10 μg) suspended in buffers of pH (7.4, 6.6 and 8.2) were incubated with $^{45}Ca^{2+}$ (50 μM and 7.5 mM, respectively) in 100 μL of assay medium at 30°C for 5 sec then filtered and intravesicular radioactivity was determined as described earlier. Data are shown relative to the Ca^{2+} uptake in control BLMV (pH 7.4). Ca^{2+} entry in thapsigargin-treated, internal Ca^{2+} pool-depleted cells, suspended in buffers of pH 7.4, 6.6 and 8.2, was studied at 250 μM (HA) and 5.0 mM (LA) $[Ca^{2+}]$. The increase in $[Ca^{2+}]_i$ at pH 7.4 was set as 100%. Data shown are ±SEM for 3–4 experiments.

KCl on Ca^{2+} influx via these two components. The following data, summarized in Table 3, demonstrate that these two Ca^{2+} influx components are likely to be distinct Ca^{2+} influx pathways. (i) Treatment of BLMV with DCCD, induces a decrease in Ca^{2+} influx via the high affinity component [13, 14] without significantly affecting Ca^{2+} influx via the low affinity component. This is an important observation since it suggests that although the two Ca^{2+} influx components appear to respond similarly to changes in pH, it is likely that two distinct protein sites (i.e., with different carboxyl groups) are involved in mediating these two activities. (ii) KCl inhibits Ca^{2+} influx into BLMV via the high affinity component to a greater extent than via the low affinity component, likely due to an effect on the V_{max} of this component (*see* inset in Fig. 3). Thus, KCl induces different effects on the two Ca^{2+} influx components in BLMV. This is consistent with our previous observation in intact acini [2] demonstrating that KCl induces a decrease in the V_{max} of the high affinity component (no change in K_{Ca}) and an increase in the K_{Ca} of the low affinity site (no change in V_{max}). Thus, these results demonstrate that, both DCCD and KCl also exert differential effects on the high and low affinity Ca^{2+} influx components in BLMV.

We have previously reported that the concentrations of Ni^{2+} and Zn^{2+} required to induce a 50% decrease in Ca^{2+} influx via the high affinity component in BLMV are 1.1 mM and 0.77 mM, respectively [14]. The present data demonstrate (*see* Fig. 2) that 0.32 mM Zn^{2+} and 0.25 mM Ni^{2+} are required to induce 50% inhibition of Ca^{2+} influx via the low affinity component in BLMV. Thus, the high affinity component appears to have a relatively greater sensitivity to Zn^{2+} than Ni^{2+}, while the low affinity component displays similar sensitivities to both divalent cations. Further much lower concentrations of Zn^{2+} and Ni^{2+} are required for inhibition of Ca^{2+} influx via the low affinity Ca^{2+} influx component. In aggregate the effects of DCCD, KCl, and the divalent cations on the high and low affinity Ca^{2+} influx components in BLMV strongly suggest that they are different transport pathways, likely mediated by different proteins. However, conclusive evidence that these $^{2+}$ influx pathways are different will require purification of the proteins mediating Ca^{2+} transport. Towards our efforts to purify the Ca^{2+} influx components, we have recently used this BLMV preparation to solubilize and reconstitute the high affinity Ca^{2+} influx component [14] and the data presented above will be useful in future studies to functionally characterize purified candidate proteins.

Table 3. Characteristics of the high and low affinity Ca^{2+} influx components in BLMV

	% Ca^{2+} entry	
	HA	LA
DCCD (2 mM)	53.52 ± 5.5	83.37 ± 6.99
KCl (50 mM)	52.21 ± 1.07	74.56 ± 2.65

DCCD treatment of BLMV was performed as described in Materials and Methods. $^{45}Ca^{2+}$ uptake into BLMV was assayed with 50 μM (HA) and 7.5 mM (LA) $CaCl_2$ in the medium. The activity has been expressed relative to the respective controls in each case; i.e., BLMV were treated with the vehicle, DMSO, for the DCCD treatment and an equivalent volume of buffer for the KCl treatment. In DCCD treated BLMV, the value for the HA site is significantly different from those obtained for control BLMV (0.5 ± 0.076 nmoles Ca^{2+}/mg protein/min, set as 100%) and for LA (i.e., shown in Table). Ca^{2+} influx via the low affinity component in DCCD-treated BLMV was not significantly different from that in control BLMV (9.53 ± 0.75 nmoles Ca^{2+}/mg protein/min, which was set as 100%). The activity in KCl-treated BLMV was significantly different from controls for both HA and LA.

In summary, we have demonstrated the presence of a relatively low affinity Ca^{2+} influx component in BLMV with K_{Ca} and other characteristics (e.g., IC_{50} for Ni^{2+} and Zn^{2+}, effects of pH, DCCD, and KCl), similar to that of the low affinity Ca^{2+} influx component detected in internal Ca^{2+} store-depleted parotid acinar cells (*see* Table 1). Additionally this component appears to be different from the low affinity Ca^{2+} influx component in unstimulated parotid acinar cells which is not inhibited by KCl, Zn^{2+}, La^{3+}, or Ni^{2+} [13, 17]. Our data also suggest that the low affinity Ca^{2+} influx component in BLMV is distinct from the high affinity Ca^{2+} influx component we have previously described in parotid acinar cells and BLMV. However, further studies will be required to identify the molecules mediating these Ca^{2+} influx pathways across the rat parotid gland basolateral plasma membrane.

We thank Dr. Bruce Baum for his constant encouragement and support.

References

1. Ambudkar, I.S., Hiramatsu, Y., Lockwich, T., Baum, B.J. 1993. Activation regulation of calcium entry in rat parotid acinar cells. *Crit. Rev. Oral Biol. and Med.* **4:**421–425
2. Chauthaiwale, J.V., Sakai, T., Taylor, S.E., Ambudkar, I.S. 1996. Presence of two calcium influx components in Ca^{2+} pool-depleted rat parotid acinar cells. *Pfluegers Arch.* **432:**105–111
3. Clapham, D.E. 1995. Calcium Signalling. *Cell.* **80:**259–268
4. Donnadieu, E., Trautmann, A. 1992. Calcium fluxes in T lymphocytes. *J. Biol. Chem.* **267:**25864–25872
5. Fasolato, C., Hoth, M., Matthews, G., Penner, R. 1993. Ca^{2+} and Mn^{2+} influx through receptor-mediated activation of nonspecific cation channels in mast cells. *Proc. Natl. Acad. Sci. USA* **90:**3068–3072
6. Fasolato, C., Hoth, M., Penner, R. 1993. Multiple mechanisms of manganese-induced quenching of fura-2 fluorescence in rat mast cells. *Pfluegers Arch.* **423:**225–231
7. Hiramatsu, Y., Baum, B.J., Ambudkar, I.S. 1992. Elevation of cytosolic [Ca^{2+}] due to intracellular Ca^{2+} release retards carbachol stimulation of divalent cation entry in rat parotid gland acinar cells. *J. Membrane Biol.* **129:**277–286
8. Hoth, M., Penner, R. 1992. Depletion of intracellular calcium stores activates a calcium current in mast cells. *Nature* **355:**353–356
9. Hoth, M., Penner, R. 1993. Calcium release-activated calcium current in rat mast cells. *J. Physiol.* **465:**359–386
10. Kaplan, M., Taylor, S.E., Ambudkar, I.S. 1994. G-protein and capacitatively regulated Ca^{2+} entry pathways are activated by muscarinic receptor stimulation in a human submandibular ductal cell line. *Pfluegers Arch.* **428:**439–445
11. Lockwich, T., Shamoo, A.E., Ambudkar, I.S. 1993. Calcium permeability of rat parotid gland vesicles is modulated by membrane potential and extravesicular [Ca^{2+}]. *Membr. Biochem.* **10:**171–179
12. Lockwich, T.P., Kim, I.H., Ambudkar, I.S. 1994. Temperature-dependent modification of divalent cation flux in the rat parotid gland basolateral membrane. *J. Membrane Biol.* **141:**289–296
13. Lockwich, T., Mertz, L.M., Ambudkar, I.S. 1993. Involvement of carboxyl groups in the divalent cation permeability of rat parotid gland basolateral plasma membrane. *Mol. Cell. Biochem.* **126:**143–150
14. Lockwich, T.P., Chauthaiwale, J., Ambudkar, S.V., Ambudkar, I.S. 1995. Reconstitution of a passive Ca^{2+} transport pathway from the basolateral plasma membrane vesicles of rat parotid gland acinar cells. *J. Membrane Biol.* **148:**277–285
15. Merritt, J.E., Rink, T.J. 1987. Regulation of cytosolic calcium in fura2-loaded rat parotid acinar cells. *J. Biol. Chem.* **262:**4958–4960
16. Mertz, L.M., Baum, B.J., Ambudkar, I.S. 1990. Refill status of the agonist-sensitive Ca^{2+} pool regulates Mn^{2+} influx in parotid acini. *J. Biol. Chem.* **265:**15010–15114
17. Mertz, L.M., Baum, B.J., Ambudkar, I.S. 1992. Membrane potential modulates divalent cation entry in rat parotid acini. *J. Membrane Biol.* **126:**183–193
18. Muallem, S. 1989. Calcium transport pathways of pancreatic acinar cells. *Ann. Rev. Physiol.* **51:**83–105
19. Muallem, S., Pandol, S.J., Beeler, T.J. 1989. Modulation of agonist-stimulated calcium influx by extracellular pH in rat pancreatic acini. *Am. J. Physiol.* **257:**G917–924.
20. Penner, R., Matthews, G. Neher, B. 1988. Regulation of calcium influx by second messengers in rat mast cells. *Nature* **334:**499–504
21. Petersen, O.H., Gallacher, D.V. 1988. Electrophysiology of pancreatic and salivary acinar cells. *Ann. Rev. Physiol.* **50:**65–80
22. Putney, J.W. Jr. 1986. Identification of cellular activation mechanisms associated with salivary secretion. *Ann. Rev. Physiol.* **48:**75–78
23. Putney, J.W. Jr., Bird, G.S. 1993. The inositol phosphate-calcium signalling system in nonexcitable cells. *Endocr. Rev.* **14:**610–631
24. Zhang, G.H., Melvin, J.E. 1993. Membrane potential regulates Ca^{2+} uptake and inositol phosphate generation in rat sublingual mucous acini. *Cell Calcium* **14:**551–556